



HAL
open science

Consecutive reactions of aromatic-OH adducts with NO, NO₂ and O₂: benzene, naphthalene, toluene, m- and p-xylene, hexamethylbenzene, phenol, m-cresol and aniline

R. Koch, R. Knispel, M. Elend, M. Siese, C. Zetzsch

► **To cite this version:**

R. Koch, R. Knispel, M. Elend, M. Siese, C. Zetzsch. Consecutive reactions of aromatic-OH adducts with NO, NO₂ and O₂: benzene, naphthalene, toluene, m- and p-xylene, hexamethylbenzene, phenol, m-cresol and aniline. *Atmospheric Chemistry and Physics*, 2007, 7 (8), pp.2057-2071. hal-00296202

HAL Id: hal-00296202

<https://hal.science/hal-00296202>

Submitted on 18 Jun 2008

HAL is a multi-disciplinary open access archive for the deposit and dissemination of scientific research documents, whether they are published or not. The documents may come from teaching and research institutions in France or abroad, or from public or private research centers.

L'archive ouverte pluridisciplinaire **HAL**, est destinée au dépôt et à la diffusion de documents scientifiques de niveau recherche, publiés ou non, émanant des établissements d'enseignement et de recherche français ou étrangers, des laboratoires publics ou privés.

Consecutive reactions of aromatic-OH adducts with NO, NO₂ and O₂: benzene, naphthalene, toluene, m- and p-xylene, hexamethylbenzene, phenol, m-cresol and aniline

R. Koch^{1,2}, R. Knispel¹, M. Elend¹, M. Siese^{1,2}, and C. Zetzsch^{1,2}

¹Fraunhofer-Institute of Toxicology and Experimental Medicine, Hannover, Germany

²Atmospheric Chemistry Research Laboratory, University of Bayreuth, Germany

Received: 26 June 2006 – Published in Atmos. Chem. Phys. Discuss.: 9 August 2006

Revised: 22 February 2007 – Accepted: 5 April 2007 – Published: 25 April 2007

Abstract. Consecutive reactions of adducts, resulting from OH radicals and aromatics, with the tropospheric scavenger molecules O₂, NO and NO₂ have been studied for benzene, naphthalene, toluene, m- and p-xylene, hexamethylbenzene, phenol, m-cresol and aniline by observing decays of OH at temperatures where the thermal back-decomposition to OH is faster than 3 s⁻¹, typically between 300 and 340 K. The experimental technique was resonance fluorescence with flash photolysis of water as source of OH. Biexponential decays were observed in the presence of either O₂ or NO, and triexponential decays were obtained in the presence of NO₂. The kinetic analysis was performed by fitting the relevant rate constants of the reaction mechanism to whole sets of decays obtained at various concentrations of aromatic and scavenger. In the case of hexamethylbenzene, the biexponential decays suggest the existence of the ipso-adduct, and the slightly higher necessary temperatures show that it is even more stable.

In addition, smog chamber experiments at O₂ concentrations from atmospheric composition down to well below 100 ppm have been carried out for benzene, toluene and p-xylene. The drop of the effective rate constant of removal by OH occurs at reasonable O₂ levels, given the FP/RF results. Comparison of the adduct reactivities shows for all aromatics of this study that the reaction with O₂ predominates over that with NO₂ under all tropospheric conditions, and that a reaction with NO may only occur after the reaction with O₂.

1 Introduction

Aromatic hydrocarbons are a major class of anthropogenic compounds emitted to the troposphere. Despite emission control measures, they still account for 20 to 30% of the

Correspondence to: C. Zetzsch
(cornelius.zetzsch@uni-bayreuth.de)

non-methane hydrocarbons in urban air (see Chapter I of the monograph by Calvert et al. (2002)). As they react rapidly with OH radicals, they have a strong influence on urban air quality. Their high ozone creation potential is not yet fully understood and justifies further work on their degradation mechanism (Jenkin et al., 2003; Bloss et al., 2004). This paper summarises our work on the consecutive steps of OH-initiated degradation of aromatic compounds in the presence of the typical atmospheric radical scavengers NO, NO₂ and O₂ and presents such data on hexamethylbenzene in the presence of O₂.

The hydroxyl initiated degradation of aromatics and the respective reaction mechanisms have been studied using various experimental techniques (see reviews by Atkinson, 1989, 1994; and Atkinson and Arey, 2003). The kinetics attributed to the formation of the addition complex, the equilibrium between the adduct, aromatic-OH, and the reactants, and the abstraction of an H atom from the aromatic ring or from a substituent, i.e. Reaction (1/–1) and (2), have been observed over a wide range of temperature and pressure. They have been studied in our laboratory as well (Wahner and Zetzsch, 1983; Rinke and Zetzsch, 1984; Witte et al., 1986) and are fairly well understood.

Addition of OH occurs preferably to a non-substituted position, and for the aromatics studied in the gas phase, ipso addition of OH, i.e. to a substituted position of the ring, is generally considered to be unimportant (Calvert et al., 2002). This minor channel has been discussed recently for the methylated benzenes by Johnson et al. (2005) with respect to combined DFT and statistical calculations for toluene. These gave 3% ipso, and no evidence was found accordingly in their UV spectra of the OH-adducts of toluene, the xylenes and 1,3,5-trimethylbenzene. There are examples of ipso addition of OH to non-fully substituted aromatics in the liquid phase: Richter and Waddell (1983) found OH addition ipso to the OH groups of protonated dopamine (4-(2-aminoethyl)-1,2-benzenediol), leading to elimination

of H₂O. Hübner and Roduner (1999) studied hydroxylation of p-methoxy-benzenesulphonate and observed various phenoxyl radical anions, i.e. the ether link was broken. Also at an ether position was the ipso addition of ¹⁸OH to the 2,4-dichlorophenoxyacetate ion studied by Peller et al. (2003), leading to a fairly complete elimination of the oxyacetate substituent. An ipso-to-methyl addition on p-cresol was found by Schuler et al. (2002) to occur with a probability of 12%, forming 4-hydroxy-4-methyl-2,5-cyclohexadiene-1-one as a final product. Ipso-addition to the OH position was confirmed to form phenoxyl radicals by eliminating H₂O. Finally, ipso-addition of OH to toluene, o- and p-cresol has been observed by Albarran and Schuler (2005) to occur at the methyl positions with yields of about 10% of the total addition and to produce the o- and p-dienones, where the latter studies used ferricyanide as an efficient scavenger of the OH adducts. No information on ipso attack was found in the literature on aniline, where according to Solar et al. (1986) a portion of 37% of the OH abstracts a H atom from the NH₂ group to produce the anilino radical, 54% go to the o-positions and another 10% to the p-position, though m- and ipso additions were not excluded. It is not clear whether such numbers – several of them are dependant on the type and concentration of scavenger – are applicable to the gas-phase processes with different scavengers.

Nevertheless, triexponential fits (Koch and Zetzsch, 2006) to OH decays in the presence of 1,3,5-trimethylbenzene obtained with FP/RF by Bohn and Zetzsch (2000) in the absence of a scavenger indicated ipso addition as does the high OH reactivity of hexamethylbenzene (HMB) of $1.1 \times 10^{-10} \text{ cm}^3 \text{ s}^{-1}$ found by Berndt and Böge (2001a) and contrasting with an extrapolated value of $6 \times 10^{-13} \text{ cm}^3 \text{ s}^{-1}$ per –CH₃ group recommended by Atkinson (1989) at 298K on the basis of consistent observations on toluene, toluene-d₅ and the three xylenes between 450 and 1150 K. Furthermore, Berndt and Böge (2001a) observed hexamethyl-2,4-cyclohexadienone as a product of ipso addition to hexamethylbenzene in the gas phase, as confirmed by the later studies by Schuler et al. (2002) on p-cresol and by Albarran and Schuler (2005) on toluene, o- and p-cresol in the aqueous phase. Therefore, we searched for biexponential decays of OH in the presence of HMB by raising the temperature in our experiment in order to detect OH released from the unimolecular decay of ipso adducts at long reaction times. A very recent study by Raff and Hites (2006), brought to our attention by one of the referees, observed brominated phenols as products from an addition of OH in the gas phase to brominated diphenylethers as another hint at ipso addition and subsequent splitting of the aromatic ether bond.

Of major interest in tropospheric chemistry, however, is the competition of the consecutive reactions of the adducts with scavenger molecules, such as NO, NO₂, O₂ and other atmospheric constituents, the possible reaction pathways and resulting product distributions. These aspects have been studied by laser photolysis/laser absorption and laser pho-

tolysis/UV absorption by Zellner et al. (1985), Bohn and Zetzsch (1999), Bohn (2001), Johnson et al. (2002, 2005), Raoult et al. (2004) and Grebenkin and Krasnoperov (2004); by discharge-flow/laser induced fluorescence (Goumri et al., 1990); in flash photolysis/resonance fluorescence studies by Perry et al. (1977), Zetzsch et al. (1990) and Knispel et al. (1990) for benzene, toluene and phenol; and in product studies by Atkinson et al. (1989), Atkinson et al. (1991), Atkinson and Aschmann (1994), Klotz et al. (1998), Smith et al. (1998, 1999), Bethel et al. (2000), Berndt and Böge (2001a, 2001b, 2003, 2006) and Volkamer et al. (2002a,b), Klotz et al. (2002), Olariu et al. (2002), Zhao et al. (2005) and Coeur-Tourneur et al. (2006) for benzene, toluene, o-, m- and p-xylene, 1,2,3-, 1,2,4- and 1,3,5-trimethylbenzene, HMB, phenol and o-, m- and p-cresol.

In the following, we present a kinetic study of the consecutive reactions of aromatic-OH adducts in the presence of variable amounts of either NO, NO₂ or O₂. Most of the results on benzene, toluene, p-xylene, phenol and m-cresol were obtained using the VUV flash photolysis/resonance fluorescence (FP/RF) technique, introduced by Stuhl and Niki (1972). The data on benzene, toluene and phenol have been reported previously (Knispel et al., 1990), but some of those measurements (benzene-OH and toluene-OH + O₂ and phenol-OH + NO₂) have been re-evaluated using improved software-tools (Koch, 1992). The data on p-xylene, m-xylene, m-cresol and aniline have been briefly reported by Koch et al. (1994) and Zetzsch et al. (1997) and are described in more detail in the present study. The measurements on HMB-OH + O₂ have been performed recently after reinstallation of the apparatus at the University of Bayreuth. The adduct reaction was furthermore examined by a smog chamber technique in N₂ with continuous addition of O₂ (Elend and Zetzsch, 1992) for benzene, toluene and p-xylene.

2 Methods

2.1 Flash photolysis/resonance fluorescence setup

The basic components are a flash lamp, a resonance lamp and a fluorescence detector mounted at right angles to each other. Photolysis of H₂O is used to produce OH since H₂O is inert against OH, enabling us to obtain long observation times of OH at low levels of the reactants in order to detect the OH adducts from their decomposition. In the following description, emphasis is on improvements (Koch, 1992) of both the set-up and evaluation procedure over what has been used by Wahner and Zetzsch (1983) and Witte et al. (1986).

2.1.1 Data acquisition and hardware

A multichannel scaler board (EG&G Ortec, model ACE MCS) with 4096 channels is used on a PC, which also controls the triggering of the flash lamp and the flows, pressures and temperatures of the experiment. The PC is equipped with

a multi-I/O card (Meilhaus PC30, 16x 12-bit A/D, 4x D/A, 24 bit I/O) supplemented by a card with 8 D/A converters (Bockstaller, PC8408). Since multiplexing the temperature signals at the sensor level proved to be unreliable, separate converter modules (Analog Devices, 5B34) for each Pt100 resistor were multiplexed at the 5-V level (Analog Devices, 5B02).

2.1.2 Software running the experiment

A TurboPascal (Borland) program was developed featuring: low-level control of the hardware; calculation of the settings necessary for intended concentrations in the cell and *vice versa*, applying calibration data for each device as well as Antoine constants for the partial pressure in the saturators; graphical presentation of the decay while it is summed up, together with a preliminary exponential fit; a user interface allowing the operator to change all the settings interactively; a batch language with one command for each menu entry of the user interface and directives for calling subroutines, i.e. other batch files, for the convenient programming of measurement tasks. Batch processing can be interrupted at any level of nested subroutines and can be resumed after a problem has been fixed or continued with the current batch file adapted to the latest findings.

2.1.3 Precautions for semivolatile compounds and a wider temperature range

To avoid condensation of low-reactivity, low-vapour-pressure compounds, the glass tubing from the thermostated saturator to the cell was heated up to and including the needle valve where the gas expands from atmospheric to cell pressure. The black anodized surface of the cell and the flanges has been removed where it prevented gas-tight contact to o-rings, lowering the leakage rate of the cell to 0.25 mbar ml/min, 0.2 ppm of the typical buffer-gas flow. Viton o-rings, degassing reactive compounds at high temperatures, were replaced by odorless silicone-rubber o-rings (Busak + Luyken) leading to longer lifetimes of OH.

2.1.4 Modifications of the flash lamp

A quartz lens (Heraeus, Suprasil, $f_{\text{vis}}=50$ mm), mounted 9 cm from the spark, focuses the VUV flash to a point well before the MgF₂ entrance window. The aim was not to increase the radical concentration (see below) but to widen the beam inside the cell: The volume, where H₂O is photolysed, is wider than the field of view of the multiplier so that the influence of diffusion and the slow flow through the cell on the decay rates can be neglected during the first second after the flash at the typical total pressure of 130 mbar. A cuvette may be placed at the intermediate focus in order to filter the VUV flash-light. This option was used in the case of p-xylene where an interfering fluorescence signal lasting several milliseconds after the flash was diminished

by a 2-cm preabsorbing layer of p-xylene vapour. Most experiments were performed using a flash energy of 2 J, a few experiments (on m-xylene) were performed using an excimer laser (EMG102, Lambda Physics) at 193 nm with an energy fluence of 10 mJ/cm² instead of the flash lamp, photolysing N₂O and converting the resulting O(¹D) to OH by the rapid reaction with H₂O. The experiments with HMB were performed with a flash lamp of 0.5 J, omitting the defocusing quartz lens.

2.1.5 Measures to increase the signal intensity

The shape of the glass tube of the resonance lamp was modified to widen just above and below the $\lambda/4$ resonator, which has been silver plated for reducing losses of microwave power. The spreading plasma is concentrated towards the point of efficient light collection by increasing the pressure to several mbar, and the aperture of the lamp is approximately doubled. The four collimating and focusing lenses, two for the lamp and multiplier each, are antireflection-coated for 300 nm. The interference filter towards the multiplier has been replaced by one with a slightly wider transmission curve (FWHM, 9 nm) but considerably higher peak transmission (47% at 309 nm, Anders, Nabburg). The total effect was an increase of signal intensity from 40 to 190 kHz (10³ counts/s) at 2 J flash energy and [H₂O] = 2×10^{15} cm⁻³. Although the background increased even more (from 5 to 40 kHz), the signal-to-noise ratio improved by a factor of 1.7, allowing us to decrease the concentration of water from 3 to 2×10^{15} cm⁻³, which decreases the signal to 160 kHz. The initial OH concentration is now well below 10¹⁰ cm⁻³ at 2 J flash energy, as estimated by comparing signal intensities (corrected for fluorescence quenching by H₂O): By titrating 6×10^{11} cm⁻³ NO₂ with excess H atoms generated by 193-nm photolysis of NH₃, OH is visible over 6 orders of magnitude. Thus, build-up of reaction products, depletion of aromatics and radical-radical-reactions are all negligible.

2.1.6 Measures to stabilize the signal

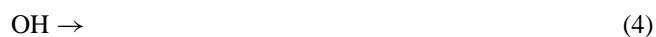
A microwave generator (Muegge, Reichelsheim, MW-GPRYJ1511-300-01, 2.45 GHz, 300 W) with a switching-mode power supply for the magnetron eliminated 100-Hz ripple, and intermittent flicker was remedied by supplying the microwave power, typically 200 W, to the lamp via a circulator (Philips, Type 2722 163 02071), absorbing the reflected power. The influence of possibly remaining low-frequency noise and drift is reduced by determining the background as close as possible to where it is needed, i.e. at the end of the decay (recorded up to 5 s). Typically, 50 to 150 scans are accumulated for a decay curve. If necessary, repeated recordings are coadded after visual inspection. The first one or two channels have to be omitted due to an afterglow/phosphorescence of the flash lamp/entrance window, lasting about 1.5 milliseconds.

2.1.7 Data reduction and evaluation

During the slow decay into the noise of the already subtracted background, binning the photon counts into the millisecond time slots of the multichannel scaler is neither necessary nor appropriate. The irrelevant high-frequency noise that is characteristic of the photon-counting technique would obscure both, low-frequency noise and signal. Even worse, in a semi-log plot, where negative values have to be omitted and small values are largely expanded, a higher density of data points would appear above the mean value and cause a systematic deviation. Therefore, the data is rebinned in a manner appropriate for decay curves that are sums of exponentials: The interval width is doubled whenever the elapsed time is 12 times the actual width, i.e. every sixth interval. By this procedure, the original 4096 data points are compressed into 62 values which are roughly equidistant on a logarithmic time scale. It has been tested by evaluation of synthetic, noisy, biexponential decays that even much coarser binning would not lead to systematic deviations. This enables us to demonstrate a dynamic range of three orders-of-magnitude in a clear plot. It should be noted that, for the fitting procedure, it is not the plotted function values of modelled decay curves that are compared to the coarsely binned data, but the integrals of the curves over the very same time intervals.

2.1.8 Reaction mechanism and kinetic analysis (FP/RF)

The following reaction mechanism, where A is the aromatic, AOH is the adduct and S is the scavenger (O₂, NO₂, or NO in this work), is considered in the resonance fluorescence experiments:



The differential equation governing the reversible formation of the adduct, AOH, with loss processes on either side of the equilibrium is given as Eq. (I):

$$\frac{d}{dt}[\text{OH}] = -a[\text{OH}] + b[\text{AOH}] \quad (\text{I})$$

$$\frac{d}{dt}[\text{AOH}] = c[\text{OH}] - d[\text{AOH}]$$

The rate coefficients c and b are the rate constants for adduct formation and back-decomposition, Reactions (1/-1), while a and d additionally contain the irreversible loss processes, Reactions (2) to (6): $a=k_4+(k_1+k_2)[\text{A}]+k_3[\text{S}]$, $b=k_{-1}$, $c=k_1$

$[\text{A}]$ and $d=k_{-1}+k_5+k_6[\text{S}]$, where $[\text{A}]$ and $[\text{S}]$ are the aromatic and the scavenger concentration, respectively, and $[\text{AOH}]$ is the concentration of the thermolabile adduct, aromatic-OH. Note that $a-c=k_4+k_2[\text{A}]+k_3[\text{S}]$ describes the formal Reaction (2), comprising both the abstraction channel and the reaction of OH with possible impurities of the aromatic. Reaction (3) is used for NO or NO₂ as scavenger only, since O₂ has been tested to be pure enough not to decrease the lifetime of OH. Reaction (4) is called diffusion loss but also contains reactions of OH with background impurities of the cell as well as an offset error in $[\text{A}]$. Similarly, Reaction (5) may comprise a unimolecular isomerisation of the adduct as well as an offset error of the flow controllers employed for the scavenger or a background of O₂ from leaks.

Not considered in our model are the formation of adduct isomers of different stability and Reaction (6) being an effective loss from an equilibrium, see Discussion.

The analytic solution of Eq. (I), already given by Wahner and Zetzsch (1983), is the sum of two exponential components $I \times e^{-t/\tau}$ for each of $[\text{OH}](t)$ and $[\text{AOH}](t)$ with common parameters τ_1^{-1} and τ_2^{-1} :

$$\tau_{1,2}^{-1} = \frac{a+d}{2} \pm \sqrt{\left(\frac{a+d}{2}\right)^2 - bc} \quad (\text{IIa})$$

The ratio of the amplitudes, I_1/I_2 , for the OH part of the solution is given by

$$I_1/I_2 = \frac{(\tau_1^{-1} - d)^2}{bc} \quad (\text{IIb})$$

while for the adduct it is simply -1 .

The coefficients b and c occur in Eq. (II) only as a product. This has no effect on the evaluation of the title reactions, see Appendix.

Note that while the dependence of τ_2^{-1} on the concentration of the scavenger may appear linear for a given data set, an evaluation according to $\tau_2^{-1}=k_5+k_6[\text{S}]$ (implying the approximation $\tau_2^{-1} \approx d$) can be considerably in error, especially in the case of NO as scavenger, due to Reaction (3). The influence of k_3 on τ_2^{-1} becomes marginal as I_1/I_2 exceeds 100, but then, however, τ_2^{-1} is hardly visible in decays of OH.

2.1.9 Fitting strategy

The two exponentials are fitted simultaneously, using as fit parameters either τ_1^{-1} , τ_2^{-1} and I_1/I_2 ; or a , d and bc (the former set can be converted into the latter by inverting Eqn. (II), starting with $\tau_1^{-1}+\tau_2^{-1}$ and $\tau_1^{-1}\tau_2^{-1}$). We call such fits "e-fits". Sets of biexponential decays obtained at various concentrations of aromatic and scavenger lead to sets of a , d and bc , varying linearly with the concentrations.

We took a further step (Koch, 1992): Sets of biexponential decays were analysed simultaneously by fitting the slopes (and diffusion offsets) of a , d and bc , see Appendix, directly to the data. The Levenberg-Marquardt algorithm (see

Press et al., 1992) is employed in a comfortable Pascal program, that allows to (i) adjust the time ranges for fitting either the background or decaying parts, to (ii) e-fit decays in a batch with individual start parameters calculated from [A] and [S], and to (iii) select subsets of decays for k-fitting a bunch of model functions to them (in fact, the functions may be watched “dancing” around the data if the PC is not too fast). The result can be displayed on the screen as succession of residuals; written to a protocol file as set of rate constants with their variances and covariances, and as table of exponential parameters to be compared to the results of e-fits; and written as time profiles to a spreadsheet to be plotted. All settings are saved for the next run of the program.

The benefit of this simultaneous fit (k-fit) is greatest for decays that are not distinctly biexponential, i.e., if τ_1^{-1} and τ_2^{-1} are separated by a factor of less than, say, 3. In these cases, the exponential parameters would have large mutual covariances, i.e., different sets of parameters would describe the decay almost equally well. The k-fit avoids this covariance problem (see the Results section for an example).

Another benefit is the ease of including proper weights: Since sources of statistical error other than shot noise of photon counts have carefully been excluded, the weight of a data point (counts in a bin) is the number of scans divided by the modelled intensity (including background) integrated over that bin. The fits were rather stiff, i.e., the sum of squares raised by more than unity on small variations of the fit parameters. The resulting error limits are purely statistical and are small compared to other uncertainties.

Care has to be taken to ensure that the decays differ only in parameters included in the model. Changes in the strongly temperature-dependent back-decomposition, for example, are not treated as such, since k_{-1} is a common fit parameter. Instead, other fit parameters would be influenced due to the covariances between them. On the other hand, the k-fit copes with an unintended variation of reactant concentration, which would be a problem for the classical two-step approach (analysis of e-fit results obtained at constant [R] and varied [S]).

In the presence of NO₂, its rapid reaction with H atoms originating from the photolysis of H₂O leads to an additional OH source-term and thus to a third exponential component in the decays (see Results section).

2.1.10 Chemicals

Deionized and bidistilled water is used. Aromatics, except benzene and toluene (Rathburn, >99.8%, glass distilled grade), are obtained from Aldrich (m- and p-xylene and HMB for analysis, >99% (GC), phenol redistilled, >99%, m-cresol, 99%, aniline, glass distilled grade, >99.5% (GC)) and are dispensed by the saturator method (Wahner and Zetzsch, 1983), usually from the liquid phase except for benzene and HMB.

Since impurities are transported and concentrated by a slowly progressing solid-liquid phase-boundary, benzene has to be further purified by freeze-pump-thaw cycles, until k_{OH} becomes stable, before it is rapidly frozen for the last time.

Concentrations of the aromatics were calculated from the Antoine constants collected by Stephenson and Malanowski (1987) and chosen, depending on their k_{OH} , for τ_1^{-1} to be between 100 and 200 s⁻¹. Note that the evaluation of the title reactions (as slope of d vs. [S]) is not influenced by errors in the vapour pressure. It has been checked that photolysis is negligible by varying the flash energy between 1.6 and 5 J, without a considerable effect on decay rates.

All gases were obtained from Messer Griesheim. Oxygen (>99.998%) is used without further purification up to some 10¹⁷ cm⁻³. For the lower concentrations, needed for the phenolics, mixtures of about 2000 ppm O₂ in He were produced using flow controllers and stored in a 2-l cylinder. Up to 5 × 10¹³ cm⁻³ NO is added from a 2000-ppm mixture with Ar (specified by the manufacturer to be within ±2%) and is purified from NO₂ impurities by a FeSO₄ × 7H₂O scrubber. As determined by H-to-OH conversion, the NO₂/NO ratio decreases from about 2 × 10⁻² to below 10⁻⁴. To prevent the formation of OH from peroxy radicals in the NO experiments (the oxidation of background impurities may proceed with less O₂ than oxidation of the aromatics), the buffer gas, usually 130 mbar of Ar (>99.998%), is purified from traces of oxygen using Oxisorb (Messer Griesheim). Up to 7 × 10¹¹ cm⁻³ NO₂ is added using permeation tubes (Vici Metronics) calibrated to ±2% by monitoring their loss of mass.

2.2 Smog chamber

The removal of the aromatic-OH adducts by O₂ is investigated in a smog chamber with 2450 l volume, described by Behnke et al. (1988), at 300 K in N₂ at atmospheric pressure at O₂ levels between about 50 ppm and 21%, as briefly reported by Elend and Zetzsch (1992). The N₂ gas, taken from liquid nitrogen (Messer Griesheim), was determined by GC-ECD analysis to contain less than 10 ppm O₂. Low levels of O₂ are reached in the smog chamber by flushing the O-ring seals with N₂ from outside. OH radicals are produced by photolysis of H₂O₂ using 7 medium-pressure arc lamps (Metallogen HMI, Osram, 1200 W). H₂O₂ (Peroxid-GmbH, >80%, stabilised) is kept constant at about 500 ppb by continuously adding 1 ppm/h from an impinger, containing 98 wt-% H₂O₂ and flushed continuously. Starting from different levels, O₂ is added continuously to the chamber and determined at 30-min intervals by GC/ECD analysis of 0.2-ml gas samples (column: Chrompack CP Sil 8 CB, 25 m, 0.32 mm inner diameter, 1.27 μm film thickness). The O₂ response is calibrated by chamber runs with exponential dilution, checked for stability against an electrochemical analyser (Oxanal, Gerhard GmbH, Blankenbach) before and after each chamber run.

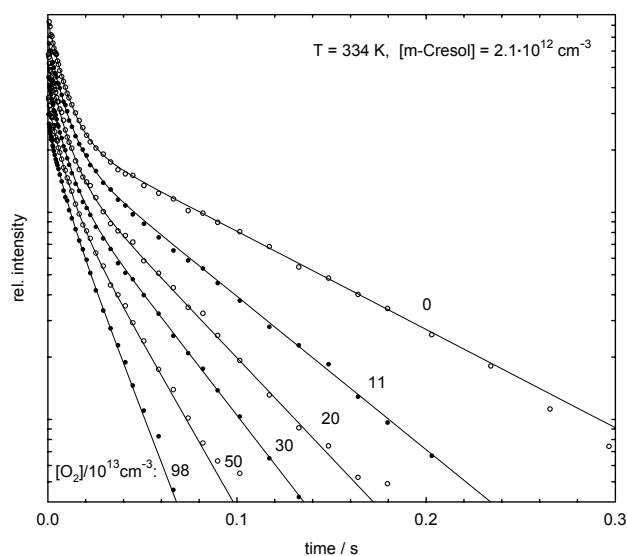


Fig. 1. Biexponential decays of OH in the presence of m-cresol and O₂ in 127 mbar of Ar at 334 K. The curves represent the result of a fit of the title reaction to 12 OH decays (these 6 and 6 similar ones), where the parameters describing the O₂-free system are fixed to values determined from another set of decays with and without m-cresol.

The aromatics and the reference compounds (n-butane, tetramethylbutane, n-heptane and the inert perfluorohexane), initially 5–40 ppb each, are determined every 30 min from 20-ml gas samples using cryogenic trapping (Nolting et al., 1988) and GC/FID (column: Chrompack Al₂O₃ PLOT).

Peak areas are divided, sample per sample, by the area of the perfluorohexane peak to correct for dilution of the chamber content during the run. The remaining decrease is obviously consumption by OH, as the [OH] profiles obtained from the reference compounds agree with each other within 5%, if the k_{OH} values 1.10 , 2.56 and $7.30 \times 10^{-12} \text{ cm}^3 \text{ s}^{-1}$ are used for tetramethylbutane, n-butane and n-heptane, respectively, which are well-established in our laboratory (Behnke et al., 1988). These values meet the recommendations of Atkinson (1994, 2003) at 300 K. Using the average [OH](t), the apparent OH rate constant of the aromatic is then calculated as a function of time and plotted against [O₂].

3 Results

3.1 Aromatic – OH + O₂

Table 1 lists the results on the eight aromatic compounds of this study. The error limits given include estimated effects of model imperfections (see below) and errors of gas flows, total pressure, and temperature. At the high O₂ levels of 10^{17} cm^{-3} needed to observe any reaction with benzene-OH, part of the VUV is absorbed between entrance window and

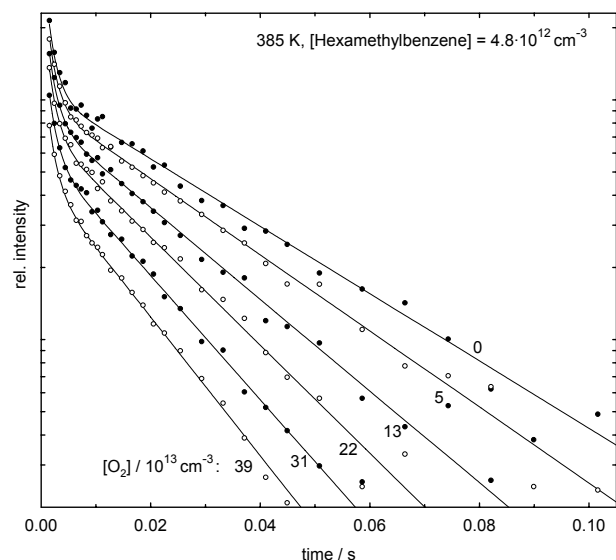


Fig. 2. Biexponential decays of OH in the presence of HMB and O₂ in 250 mbar of He at 385 K. The curves represent the result of a fit of the title reaction to 10 OH decays (these 6 and 4 similar ones at [HMB] = $1.0 \times 10^{12} \text{ cm}^{-3}$).

detection volume, adding to the gradient of [OH] _{$t=0$} due to the divergence of the beam. It has been checked that, in the absence of benzene, [OH](t) does not depend on [O₂] except for its amplitude. Oxygen atoms and ozone are formed in concentrations estimated to be negligible.

For benzene-OH, the reaction rate constant with O₂ has been obtained at four temperatures in the range 299 to 354 K. In order to keep the slow exponential component at a detectable level with decreasing temperature, the rate of adduct formation ($\approx \tau_1^{-1}$) must be reduced with the rate of its thermal back-decomposition, thus limiting the range of variation of τ_2^{-1} . For this reason and due to the quenching of the resonance fluorescence by O₂, the absolute error is higher at 299 K. How the k-fit helps to include decays with $\tau_2^{-1} \approx \tau_1^{-1}$, becomes more obvious with the stronger signals in the case of m-cresol where 10^{15} cm^{-3} of O₂ are sufficient: Fig. 1 shows decays obtained at 334 K with curves representing the result of the k-fit. Note that the two steepest decays differ considerably and therefore contain information about the target reaction, but that the steepest one would be impossible to evaluate by an e-fit due to instability (see Methods section).

Figure 2 shows the case of hexamethylbenzene, for which the temperature had to be raised by about 40 K compared to the other monoaromatics, for obtaining sufficiently biexponential decays, indicating a relatively high stability of the ipso-adduct.

Experiments had also been made with naphthalene (Koch and Zetzsch, 1994) at temperatures well above 370 K, where the OH-adduct starts to decompose on the FP/RF time-scale. These experiments suffer, however, not only from low signal

intensities due to quenching of the OH-fluorescence by O₂ but also from sticky reaction products, which increase the background reactivity of the cell and are photolysed by the flash to produce OH and other radicals (OH decays were observed with only He flowing through the cell). Recent measurements with a different flash lamp (10 instead of 50 nF capacitor, omitting the Suprasil lens and admitting the vacuum UV light down to 115 nm through the MgF₂ window for a more effective photolysis of water compared to organics) and further improved detection limit (polished microwave resonator, He instead of Ar in the lamp) yielded apparent O₂ reactivities well below the former result of Koch and Zetzsch (1994) of $1.1 \times 10^{-16} \text{ cm}^3 \text{ s}^{-1}$ and show a marked dependence on H₂O concentration, i.e. radical and product level. Thus, $k(\text{naphthalene-OH} + \text{O}_2)$ at 400 K may well be less than $10^{-17} \text{ cm}^3 \text{ s}^{-1}$, in accordance with the negative temperature dependence observed in experiments at 336 and 298 K (Koch and Zetzsch, 1994) employing cycling of radicals (Koch et al., 1994 and 1997).

3.2 Aromatic – OH + NO₂

In the presence of NO₂, the rapid reaction of H atoms (originating from the photolysis of H₂O) with NO₂ generates additional OH and leads to a third exponential component (Zetzsch et al., 1990). The model is supplemented by the H+NO₂ rate constant, $1.3 \times 10^{-10} \text{ cm}^3 \text{ s}^{-1}$ (Wagner and Welzbacher, 1976; Michael et al., 1979), plus an H-atom diffusion term, and the triexponential solution is used in the analysis. Note that in the case of NO₂ as scavenger, coefficient a contains a term proportional to [NO₂]. For the respective rate constant (OH + NO₂ + M), measurements in the absence of aromatic yielded a value of $k_3 = 2.4 \times 10^{-12} \text{ cm}^3 \text{ s}^{-1}$ at 133 mbar in Ar at 319 K, in good agreement with the literature (Paraskevopoulos and Singleton, 1988).

For most aromatics, the model matches the shape of the observed OH time profiles quite well, see for example Fig. 2 in our previous paper (Knispel et al., 1990). In the case of p-xylene, shown in Fig. 3, the deviations during the first 30 milliseconds indicate a higher initial H-atom concentration. It appears that the VUV photolysis of p-xylene leads to the formation of H atoms. At $t > 60 \text{ ms}$, however, the [OH]/[AOH] ratios, which influence the effective loss rate depending on losses on both sides of the equilibrium, are thought not to be distorted by the fast H-to-OH conversion, and that part of the decays is used for a k-fit (with the parameters describing the scavenger-free system held fixed). As can be seen in Fig. 3, the model adequately describes the [NO₂]-dependence of τ_2^{-1} . The results on the six aromatic compounds studied with NO₂ are listed in Table 1.

3.3 Behaviour of the adducts in the presence of NO

For the case of NO as scavenger, the rate constant of the interfering reaction with OH is determined in the absence of

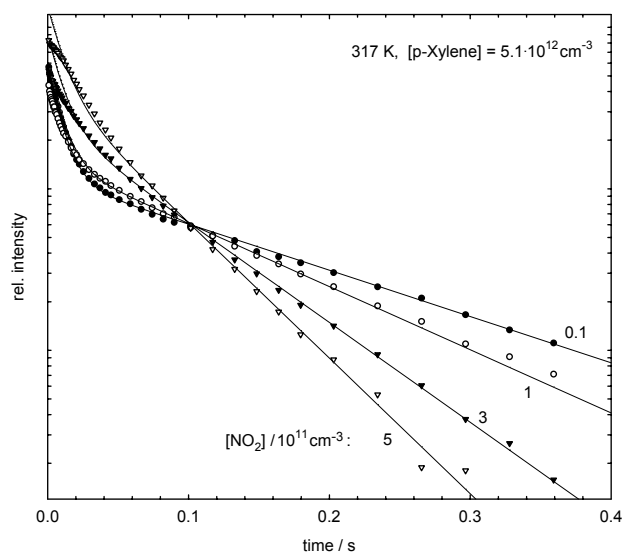


Fig. 3. Triexponential decays of OH in the presence of p-xylene ($5 \times 10^{12} \text{ cm}^{-3}$) and NO₂ in 130 mbar of Ar at 317 K. The triexponential model curves represent the result of a global fit. Obviously, the [NO₂]-dependence of the final slopes is well described by the model while the earlier parts of the decays had to be excluded from the fit (see text).

aromatics to be $k_3 = 0.95 \times 10^{-12} \text{ cm}^3 \text{ s}^{-1}$ at 320–343 K with 133 mbar of Ar as third body, in good agreement with literature data of Anastasi and Smith (1979) and reviewed by Paraskevopoulos and Singleton (1988).

In the presence of aromatics, the loss of OH increases mainly τ_1^{-1} but also τ_2^{-1} and I_1/I_2 . As a compromise between reduced influence on, and visibility of, the second exponential, the concentration of the aromatic is chosen, at any given temperature, for the adduct-to-OH ratio being about 10.

The mutual covariances of exponential parameters are avoided by the k-fit, from which 2- σ upper limits for most of the adduct+NO reactions of $3 \times 10^{-14} \text{ cm}^3 \text{ s}^{-1}$ are obtained at about 330 K. The uncertainty is about threefold higher in the cases of phenol, since the higher branching ratio for its abstraction channel limits the dynamic range of τ_2^{-1} , and p-xylene, due to the photolysis and fluorescence of the aromatic. Cycling experiments with naphthalene (Koch and Zetzsch, 1994) showed such a high yield of HO₂ that the radical loss due to adduct+NO cannot be faster than $10^{-13} \text{ cm}^3 \text{ s}^{-1}$. Generally, the influence of carefully purified NO on the loss of the adducts is very small, and the upper limits obtained from the observations with 7 aromatics are listed in Table 1.

3.4 Smog chamber

Five runs with all three aromatics (benzene, toluene and p-xylene) together, two runs with benzene and one each with toluene and p-xylene were performed at OH levels ranging

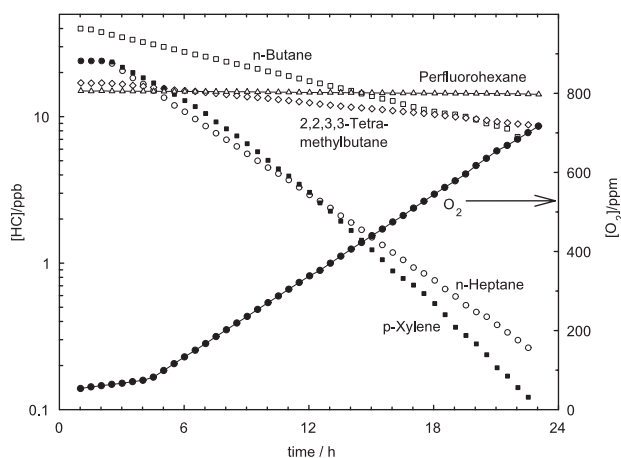


Fig. 4. Chamber experiment on p-xylene. Dilution-corrected time profiles of the organic compounds (to the logarithmic ppb scale) and [O₂] (linear ppm scale). Lights were switched on at $t=2.4$ h, and continuous addition of O₂ starts at 4.5 h. Note the curvature observed for p-xylene, indicating an O₂-dependent rate constant, in contrast to the alkanes.

from 5 to $10 \times 10^6 \text{ cm}^{-3}$. Figure 4 shows a run with p-xylene, where OH is produced from photolysis of H₂O₂ at 420 ppb. The logarithmic scale applies to the organics while the continuously added oxygen is plotted to the linear scale at the right. After an initial, linear increase of O₂ by 7.6 ppm/h (from very minor leaks and decomposition of H₂O₂), O₂ is increased by 35 ppm/h. The exponential consumption of the reference compounds indicates [OH] to be fairly constant while the consumption of p-xylene accelerates with [O₂]. The quantitative evaluation yields a time profile of [OH](t), reaching a stable level within less than a sampling period and slowly increasing from 8.3 to $8.6 \times 10^6 \text{ cm}^{-3}$ during the following 20 h.

4 Discussion

4.1 Deviations from the model and errors

No systematic deviations of the data from the biexponential curves of the k-fits were observed, and for the majority of measurements with high signal-to-noise ratio, tiny deviations from the model reach the detection limit. Those tiny model imperfections probably include the treatment of diffusion as first-order loss process, transport of the flashlamp-irradiated gas volume by the flow, temperature gradients, background reactions other than simple OH loss (such as reversible addition to trace impurities), OH sources due to ozone, radical-radical reactions, adduct isomers, equilibration of the adduct+O₂ reaction (see below), and other effects not thought of yet.

Since the typical total effect of these tiny deviations of observation from model was an increase of the sum of squares over its expectation value (= number of data points minus number of fit parameters) by only 50 to 100 percent, i.e. comparable to the low level of noise, it is impossible to discriminate between the effects even if only two or three of them are dominating. Thus, the influence of model imperfections on the evaluated rate constants could only be estimated. Although these effects should not be treated as statistical scatter, the estimated uncertainties resemble two standard deviations in the sense that we would be surprised if more than a few values will turn out to be outside of the given interval.

4.2 Adduct isomers and ipso addition

Ipsso addition may also contribute to OH decays in the presence of less substituted aromatics. Distinctly triexponential decays are possible – and have been detected (Koch and Zetzsch, 2006) in decays of OH in the presence of trimethylbenzenes (Bohn et al., 2000) – if two of the adduct-formation rate constants b_i (of an Eq. (1) supplemented for several adducts) are similarly large *and* the corresponding time constants d_i are different enough. This is not the case for the title aromatics since our simple model was sufficient to explain the decays. Without having done simulations dedicated to this question, we estimated that the spread of the d_i is less than a factor of two (for symmetrical branching – if one adduct is formed in a large excess, the deviation may be larger).

Although ipso addition of OH to HMB had been expected from the rate constant being much higher than calculated for H atom abstraction alone, it was astonishing to find the adduct even more stable than, e.g., toluene-OH, where ortho addition is known to dominate. As mentioned above, Raff and Hites (2006) found ipso addition of OH to ether positions of polybrominated diphenylethers in the gas-phase. Therefore, ipso addition should be considered at least for highly substituted benzenes.

Available computing power is increasing rapidly, but Hartree-Fock results are still too uncertain to solve the problem of aromatic oxidation. Suh et al. (2002) studied which level of theory yielded the most realistic binding energy of OH to toluene and then used the – in this sense – best level of theory to calculate rate constants. The forward reaction was overestimated by only a factor of two, which is a reasonable result for an almost barrierless addition, but the back-decomposition was about two orders of magnitude too fast. By calculating dimensionless equilibrium constants for a 1-atm partial pressure of toluene, they concluded “that unimolecular decomposition of the OH-toluene adduct is too slow to compete with bimolecular recombination”. Back-decomposition is indeed unimportant, but the competitor is the adduct+O₂ reaction.

Table 1. Rate constants, k_G , for reactions of adducts, aromatic-OH, with O₂ and NO₂ and upper limits for the reactions with NO obtained by FP/RF at various temperatures (T in K), employing flash photolysis of H₂O (>160 nm) in 130 mbar of Ar.

k (cm ³ s ⁻¹)	Benzene ^a	Toluene ^a	m-Xylene ^c	p-Xylene	Hexamethylbenzene ^d	Aniline	Phenol ^a	m-Cresol
$k_{O_2}^{add}/10^{-16}$	1.6±0.6 ^b (299)	5.6±1.5 ^b (299)	18±5 (303)	8.8±2.5 (298)		6±2 (320)	300±70 (323)	640±150 (317)
	2.1±0.4 ^b (314)	5.6±0.6 ^b (321)	16±3 (323)	8.3±2.0 (308)			260±60 (333)	750±150 (319)
	3.0±0.3 ^b (333)	5.6±0.6 (339)		8.7±1.5 (319)			270±50 ^e (337)	> 800 (324)
		5.3±0.7 (347)		7.1±1.0 (327)		15±5 (340)	290±60 (343)	820±100 (334)
	3.7±0.4 ^b (354)	5.9±0.8 (354)		8.8±1.5 (332)	1800±300 (355)	9.6±3 (350)	270±60 (353)	800±100 (350)
				1200±200 (385)		360±50 ^e (363)		
$k_{NO_2}^{add}/10^{-11}$	2.75±0.4 (305)	3.6±0.5 (300)		3.5±0.5 (317)				4±1 (317)
	2.45±0.3 (320)	3.6±0.4 (311)						4±1 (325)
	2.5±0.4 (333)	3.6±0.4 (320)		2.9±0.5 (330)		5±2 (330)	3.4±0.6 ^b (331)	
	2.5±0.4 (349)	4.0±0.6 (338)					4.1±0.7 ^b (354)	
$k_{NO}^{add}/10^{-13}$	<0.3 (319)	<0.3 (333)	<0.3 (304)	<1 (330)		<0.1 (330)	<0.7 (316-332)	<0.3 (330)

^aPublished before (Knispel et al., 1990),^bre-evaluated (Koch, 1992),^claser photolysis of N₂O at 193 nm in He,^d250 mbar of He, 0.5 J flash photolysis of H₂O at > 115 nm,^e30 to 300 mbar Ar.

4.3 Adduct reactivities

Adduct reactivities are given in Table 1. The obtained adduct+NO₂-reaction rate constants are not far from collision frequency and, therefore, do not show a significant temperature dependence. On the other hand, the obtained O₂ reactivities are much lower and span a range of three orders of magnitude, with each methyl substituent increasing the reactivity by about a factor of 3 (comparing benzene with toluene, m-xylene and finally HMB). The only cases with a significant temperature dependence are the two extreme ones, benzene and HMB, with positive and negative activation energy, respectively. The factor of 3 also occurs between the adduct reactivities of phenol and m-cresol, which are, however, more reactive than the corresponding non-phenolic cases by a factor of 200. The following comparisons with literature data are sorted by scavenger species.

4.4 Reaction of the adduct with NO

Our upper limits for the aromatic-OH+NO reactions are so low that NO cannot compete with O₂ as scavenger for the adduct. Not even in high-NO_x chamber runs, where the observed [NO] dependence of product yields is due to a different NO reaction (Klotz et al., 2002).

For the NO reactivity of benzene-OH (hydroxycyclohexadienyl, HCHD), Zellner et al. (1985) obtained a value of

1×10^{-12} cm³ s⁻¹ which should be two orders of magnitude lower to fit within our upper limit and is probably caused by NO₂ as impurity in the NO mixture, that was used without purification. This applies as well to earlier results of Witte and Zetzsch (1988) on both, benzene-OH and toluene-OH, of 6×10^{-13} cm³ s⁻¹, which were also not corrected for the influence of the OH+NO reaction.

An alternative explanation for that discrepancy has been proposed by Berho and Lesclaux (2001) who studied the corresponding benzene-H+NO-reaction by FP/UV-absorption: For both radicals, the addition of NO would be reversible and the equilibrium would change sides between the conditions of our experiment and of Zellner et al. (1985). For both radicals, however, the proposed equilibrium is problematic. For benzene-H+NO, Berho and Lesclaux (2001) noted that the obtained A-factor of the back-decomposition was unreasonably low. For benzene-OH+NO, the LP/LLPA-study on radical cycling of Bohn and Zetzsch (1999) delivered an upper limit of $< 5 \times 10^{-14}$ cm³ s⁻¹ for $k(\text{benzene-OH+NO})$. This upper limit, although somewhat higher than our FP/RF result, poses a threat to the proposed equilibrium, as the conditions (temperature, NO level) are closer to those of Zellner et al. (1985), leaving no room for the proposed change in the mechanism. Anyway, the equilibrium would be far on the left-hand side even in high-NO_x chamber experiments.

On the other hand, the NO₂-in-NO impurity may also have caused the tailing absorption observed by Berho and

Lesclaux (2001), where a fraction of the initial H atoms is converted by NO₂ into OH radicals, in competition to H+benzene – a possible reason for the [NO] dependence of the level of the background absorption. A fraction of OH adds to benzene, in competition to the OH+H₂ reaction, possibly causing the temperature dependence of the background absorption. Finally, the background absorber, benzene-OH, may have been consumed by the remaining NO₂, appearing as a slow, irreversible NO reaction (their Reaction 2b).

4.5 Reaction of the adduct with NO₂

Zellner et al. (1985) studied also the NO₂ reaction of HCHD, fitted exponentials to absorption profiles (of the adduct and possibly subsequent products at 308.5 nm) and obtained a rate constant which is a factor of 3 below the result of this study. Goumri et al. (1990) report a value of $(4\pm 2)\times 10^{-11}\text{ cm}^3\text{ s}^{-1}$ for toluene-OH at 297 K in good agreement with the present study, and Bjergbakke et al. (1996) a value of $(1.1\pm 0.2)\times 10^{-11}\text{ cm}^3\text{ s}^{-1}$ for HCHD at 338 K. In the latter study, the radical level was so high that almost half of the initial 0.2 mbar NO₂ were consumed and their stated observation of the peroxy radical has already been disputed (Koch, 1997).

4.6 The adduct reaction with O₂

In an additional measurement, Zellner et al. (1985) switched the bath gas (20 mbar) from N₂ to O₂ and found a slight decrease of the slope of τ_2^{-1} vs. [NO] which could be explained by cycling of OH via HO₂ from benzene oxidation. However, instead of an increased offset, τ_2^{-1} at [NO]=0, hinting at an O₂ reaction, they mention very slow decays even at 50 mbar of O₂. Based on that paper, Atkinson et al. (1989) estimated an upper limit of $2\times 10^{-16}\text{ cm}^3\text{ s}^{-1}$, just including our result. Another experiment less than a factor of 2 off the goal to detect a slow O₂ reaction is that of Perry et al. (1977), who expressed their result on toluene-OH as being less than $1.0\times 10^{-15}\text{ cm}^3\text{ s}^{-1}$ at 353–397 K. More recently, several authors studied the transient absorption of HCHD in the presence of O₂ (Bohn and Zetzsch (1999), Johnson et al. (2002), Raoult et al. (2004), Grebenkin and Krasnoperov (2004)). Bohn and Zetzsch (1999) provided first evidence of a fast equilibrium (7/–7) in the gas phase, predicted theoretically by Lay et al. (1996) and Ghigo and Tonachini (1998) but already observed in water by Pan and Von Sonntag (1990).



Bohn and Zetzsch (1999) observed a decrease of the HCHD signal with O₂ and a saturation of Reaction (6), which is now an effective loss term covering reactions competing with Reaction (7) or (–7).

Should this equilibrium be included in modelling the decays of this work? For benzene the equilibrium constant is known to be so small that the equilibrium is far on the

left-hand side. Although k_{-7} is somewhat uncertain, it is much faster than k_{-1} so that the steady-state approximation can be used to derive what is already obvious from Fig. 4 of Bohn and Zetzsch (1999): The saturation effect of the equilibrium on the effective rate constant k_6 is negligible under our conditions (about 1% for benzene at 299 K, even less at higher temperatures, similar for toluene, where, according to Bohn (2001), K_{eq} is only slightly larger). For the other aromatics of this study, the peroxy radical may be more stable, but also less O₂ was needed in the experiments. Anyway, no saturation effects have been detected in our experiments.

The effective k_6 of $5.5\times 10^{-16}\text{ cm}^3\text{ s}^{-1}$ obtained by Johnson et al. (2002) is considerably higher than observed in this work, $1.6\times 10^{-16}\text{ cm}^3\text{ s}^{-1}$, and by Bohn and Zetzsch (1999), $2.1\times 10^{-16}\text{ cm}^3\text{ s}^{-1}$. Improvements of the apparatus of Johnson et al. (2002) by Raoult et al. (2004) allowed the use of lower radical concentrations which resulted in slower decays, corresponding to $k_6=2.5\times 10^{-16}\text{ cm}^3\text{ s}^{-1}$. These discrepancies are obviously due to radical-radical reactions.

Very recently, Grebenkin and Krasnoperov (2004) obtained similarly shaped and timed decays, but proposed a radical-radical Reaction (8) instead of Reaction (6) to explain the increased loss rate with added O₂:



Although they do not rule out Reaction (6), they denigrate it for the lack of a plausible mechanism for a reaction being both rather slow and almost independent of temperature. Under our experimental conditions on the left-hand side of (7/–7), however, their loss mechanism would lead to a strongly negative temperature dependence of the effective loss rate (due to the positive activation of Reaction (–7) diminishing RO₂, a reactant of Reaction (8)) in contradiction to the slightly positive temperature dependence obtained for benzene, see Table 1.

Note also that a loss due to Reaction (8) would not saturate at high O₂ concentrations, as observed by Bohn and Zetzsch (1999), but would go through a maximum at the point where $[\text{HCHD}] = [\text{RO}_2]$. Although Grebenkin and Krasnoperov (2004) reach such conditions by their variation of temperature, they did not vary the O₂ concentration. They are right in stating that Reaction (6) is not needed to model their data, but this is not a result but a limitation of their experiment: It is hard to estimate to what extent their decays, recorded not far enough into the uncertain background, are hyperbolic due to Reaction (8) or exponential due to a pseudo-first-order reaction as Reaction (6).

The parameter describing the possible influence of radical-radical reactions on the evaluation of k_6 is not the radical level itself but the radical-to-oxygen ratio. That ratio is much lower in our FP/RF experiments than in the experiments of Grebenkin and Krasnoperov (2004) and of Johnson et al. (2002) and Raoult et al. (2004) but even lower in the absorption experiments of our laboratory (Bohn and Zetzsch, 1999). In that experiment, however, an underlying

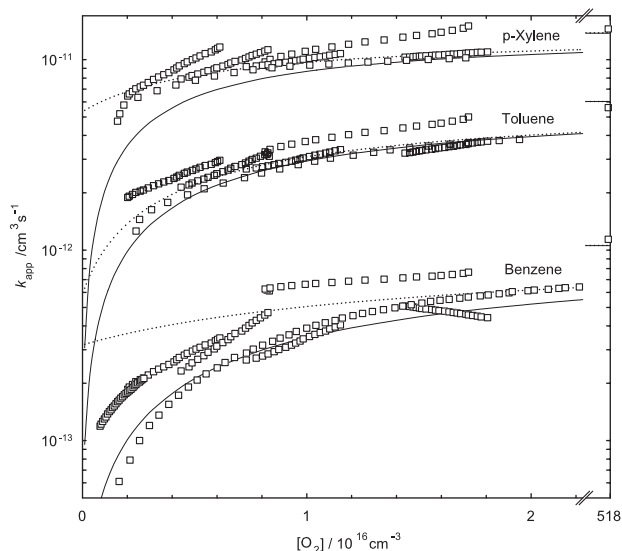


Fig. 5. Rate constants for the removal of aromatics by OH in nitrogen as a function of $[O_2]$ up to atmospheric composition, 300 K, 1 bar. Model curves are calculated according to Eq. (III) using rate constants obtained with FP/RF (see text).

background absorption with unknown formation kinetics has been subtracted, influencing the simultaneous determination of k_6 and the equilibrium constant (7/–7).

The result obtained by Bohn (2001) for toluene, $(6.0 \pm 0.5) \times 10^{-16} \text{ cm}^3 \text{ s}^{-1}$, is in excellent agreement with this work, that is further confirmed by Johnson et al. (2005).

4.7 Smog chamber experiments and product studies

The radical-to-oxygen ratio is difficult to estimate for our chamber experiments. In Fig. 5, the apparent rate constant for removal of the aromatic by OH, k_{app} , is plotted for all the runs of this study together with model curves calculated according to Eq. (III), where the addition channel is reduced by the back-decomposition competing with O₂,

$$k_{\text{app}} = k_2 + k_1 / (1 + k_{-1} / k_6 [O_2]) \quad (\text{III})$$

using FP/RF results for adduct formation and back-decomposition and either (solid lines) reasonable values for the abstraction channel derived from our FP/RF data plus literature data at higher temperatures, or (dotted lines) the total loss observed in the FP/RF experiments exceeding reasonable values for diffusion (see Appendix).

Although the downward trend of k_{app} with decreasing O₂ follows the model curves and reaches, in the case of benzene, a fairly low value, the data is obviously less reproducible than could be expected from the accurate sample analysis. While the determination of $[O_2]$ apparently contributes to the scatter at low concentrations of O₂, this is unlikely to be significant above 10^{16} cm^{-3} . The additional

Table 2. Scavenging by NO₂ calculated from FP/RF data and observed in smog chambers for the OH-adducts of benzene, toluene, p-xylene, and phenol.

Aromatic	$[NO_2]_{1/2}(\text{ppm})$	
	FP/RF	Chamber
Benzene	1.3	1.4 ^{a,b} Volkamer et al. (2002a)
Toluene	3.3	^b
p-Xylene	5.1	4.3 Bethel et al. (2000)
Phenol	160	29 Berndt and Böge (2003)

^aVolkamer, private communication (2007): The data from Fig. 6 in Volkamer et al. (2002a) show a 50% NO₂ effect at 1.1 ppm. Furthermore, the equilibrium (7/–7) buffers some sensitivity towards NO₂, leading to a value of 1.4 ppm. ^bSee also discussion by Atkinson and Aschmann (1994).

loss processes may well be reactions of the adduct with peroxy radicals. While the level of OH radicals is only slightly higher than outdoors, the level of peroxy radicals may exceed the value of 10^8 cm^{-3} observed in the remote boundary layer (Monks et al., 1998) by a factor of ten, since in our chamber, background NO_x is even lower. Thus, the ratio may be similar as in our FP/RF experiments, but another factor of about three should be applied to compare the steady-state concentration in the chamber with the initial concentration of the pulsed experiments. While our chamber experiments do show the drop of the apparent OH reactivity at the right range of O₂ concentrations, a heated chamber would allow experiments at higher O₂ concentrations or with more reactive adducts than benzene-OH, due to the accelerated thermal back-decomposition of the adduct.

The competition of O₂ with NO₂ takes place on an even faster time scale. In the lower troposphere, the lifetime of the adduct with respect to the effective O₂ reaction is of the order of a millisecond for benzene and even less for the substituted aromatics. As the equilibrium of the adduct with the peroxy radical causes not only a saturation effect of the scavenging by O₂ but also lowers the rate of the NO₂ reaction, one can still use the ratio of the two rate constants to calculate the level of NO₂, $[NO_2]_{1/2}$, where half of the adducts are scavenged by NO₂ instead of O₂. While tropospheric NO₂ levels (averaged over the region of benzene oxidation) are much lower than the 1.3 ppm value calculated for benzene, scavenging by NO₂ becomes important in high-NO_x chamber experiments.

Table 2 compares the $[NO_2]_{1/2}$ -levels calculated from Table 1 with values fitted to NO₂-dependent product yields of chamber experiments of Volkamer et al. (2002a, yields of phenol from benzene – considering that the reaction of NO₂ with AOH has been determined by the spectroscopic quantification of Klotz et al. (2002) to deliver 6% of phenol from benzene), Bethel et al. (2000, yields of 3-hexene-2,5-dione

from p-xylene), and Berndt and Böge (2003, yields of catechol from phenol decreasing from 73% in the absence to 35% at high NO₂), respectively. The agreement is excellent, except for phenol, where the chamber data imply a fivefold higher efficiency of NO₂. Note that the situation in high-NO_x chamber experiments is more complicated than suggested by tabulating [NO₂]_{1/2} values, as NO may open another exit channel from the equilibrium: The RO₂+NO reaction probably contributed to the observed NO dependencies of [benzene-OH](*t*) (Bohn and Zetsch, 1999) and of product yields from benzene (Klotz et al., 2002), but was disregarded by Suh et al. (2003) who theoretically studied the competing isomerization reaction.

Very recently, the large yield of phenol (53%) from benzene in the absence of NO₂, reported by Volkamer et al. (2002a), has been confirmed by Berndt and Böge (2006), reporting 61%. The observation of a yield of 24% phenol in the presence of NO₂ at 9.6 ppm by Atkinson et al. (1989) would not be too far from the expected decrease with NO₂, though it is in contradiction to direct observations by Klotz et al., 2002, who find lower phenol yields even under conditions where most AOH reacts with NO₂. Possible reasons for this discrepancy have been discussed by Klotz et al. (2002) and are not repeated here. The yields of phenolic products from the methylated benzenes toluene, p-xylene and 1,3,5-trimethylbenzene are known to increase with NO₂, and a yield of 45% of 2,5-dimethylphenol from p-xylene-OH with NO₂ has been reported by Volkamer et al. (2002b). Atkinson and Aschmann (1994) observed a decrease of the yield of 2,3-butanedione from o-xylene with the expected curvature and a [NO₂]_{1/2} value of about 2 ppm, confirmed by an experiment with fivefold decreased level of O₂ (RO₂ from the equilibrium (7/-7), see Volkamer et al. (2002b). The decreasing yields of 2,3-butanedione from 1,2,3-trimethylbenzene and 1,2,4-trimethylbenzene with increasing NO₂ observed by Bethel et al. (2000) can be taken as a hint at a similar competition of NO₂ with O₂ in the reaction with the OH-adducts.

5 Conclusions

The present work shows that ipso addition of OH should be considered for higher methylated benzenes and that the only relevant atmospheric scavenger for aromatic-OH adducts is O₂. While the adduct+NO reaction can be neglected even under high-NO_x simulation-chamber conditions, NO₂ levels near 1 ppm should be avoided in chamber experiments aimed at the mechanism of tropospheric aromatic oxidation. It is clear from the data in Table 2 that a few 100 ppb of NO₂ are enough to change the oxidation mechanism of aromatics substantially, and the oxidation pathways of benzene are affected by almost 10 % at the 200 ppb level of NO_x. Though such levels can occur under very polluted conditions in megacities, chamber experiments must be carefully

designed by varying NO_x over a relevant range in order to determine atmospheric oxidative capacity and to represent feedback and the formation of secondary pollutants.

The mechanism of the effective Reaction (6) is still unclear. The low pre-exponential factor of about $5 \times 10^{-14} \text{ cm}^3 \text{ s}^{-1}$ obtained in this work indicates a narrow transition state. The formation of phenolics + HO₂, favoured by Raoult et al. (2004) to be direct rather than subsequent to Reaction (7), is not of that kind. Another loss process contributing to *k*₆ could be an unimolecular reaction in competition to Reaction (-7), e.g. the isomerisation to a bicyclic radical. This must immediately form HO₂ since a high yield of prompt HO₂ is observed in our FP/RF experiments employing cycling of radicals (Koch et al., 1994 and 1997). Such a release of HO₂ radicals has been observed in aqueous-phase reactions of O₂ with a large number of OH-adducts (Fang et al., 1995) including toluene-OH, benzene-OH (Pan et al., 1993) and phenol-OH (Mvula et al., 2001) and awaits to be studied in the gas phase in the absence of NO_x. The almost temperature-independent yield of phenol from benzene, determined between 286 and 306 K by Volkamer et al. (2002a) and the enthalpy data of Lay et al. (1996), scaled to the experimental value for *k*₇/*k*₋₇ by Bohn and Zetsch (1999), imply that the direct channel contributes a fraction of 0.8 to the effective Reaction (6) and that the isomerisation of the bicyclic peroxy radical, releasing HO₂ amounts to a fraction of 0.2, see Volkamer et al. (2002a). Further studies are required to determine the extent of OH recycling in the presence of O₂ and NO and to resolve the radical budget with respect to the ozone creation potential of aromatics in the troposphere.

Appendix A

The coefficients *a*, *d* and *b* · *c* can be split into three terms according to their concentration dependence:

$$a = a_0 + a_A[A] + a_S[S] \quad (\text{A1})$$

$$b \cdot c = bc_A[A] \quad (\text{A2})$$

$$d = d_0 + d_A[A] + d_S[S] \quad (\text{A3})$$

To each group of biexponential decay curves (*p*,*T*=const; [A], [S] variable), a set of effective rate constants: *a*₀, *a*_A, *a*_S, *bc*_A, *d*₀, *d*_S is fitted simultaneously. Thereby *a*₀=*k*₄, *a*_S=*k*₃ and *d*_S=*k*₆ result directly from the evaluation; any reaction of the adduct with the aromatic (*d*_A) turns out to be insignificant. The three constants *a*_A=*k*₁+*k*₂, *bc*_A=*k*₁*k*₋₁ and *d*₀=*k*₋₁+*k*₅ contain four degenerate rate constants. This degeneracy can be overcome by considering the limiting cases at low and high temperature, and assuming Arrhenius behaviour for the abstraction, the addition and the unimolecular decay (*k*₁, *k*₋₁, *k*₂), for the diffusion of OH (*k*₄) and for the diffusion of the adduct (*k*₅). The quantity *k*₅, termed adduct diffusion, includes any other thermal loss

of the adduct, AOH, such as isomerisation and other reaction channels not leading back to OH. Likewise, the quantity k_2 , termed abstraction, may include any impurity of the aromatics.

The coefficients b and c occur only as a product in Eq. (II) with the consequence that, by observing OH alone, there remains an uncertainty about the assignment of observed radical loss to the two sides of the equilibrium connected with a tradeoff between b and c (the product bc is determined by the data): If all the loss is due to the processes denoted Reaction (2), decreasing the contribution of c to the slope of coefficient a versus [aromatic], then c is small and b is as large as possible, $b = d$ in the absence of any scavenger. On the other hand, the loss may be assigned to processes competing with the back-decomposition of the adduct, i.e. Reaction (5) denoted adduct diffusion. In this case, the contribution of b to d decreases while c increases. Note that in the case of added scavenger, b contributes to the *offset* of d only, while the evaluation of the target reaction (k_6 =*slope* of d) is not affected. Note also that the coefficients b and c , and thus the equilibrium constant, would only be separable if one could measure absolute concentrations of both OH and the adduct (b occurs without an accompanying factor c in the adduct-to-OH ratio).

Acknowledgements. Support of this study by the Federal Ministry for Research and Technology (grant 07 EU 705), and the Commission of the European Communities (grants STEP 0007-C and RII3-CT-2004-505968-EUROCHAMP) and the Federal Ministry of Environment is gratefully acknowledged. We thank the referees and B. Bohn and R. Volkamer for the stimulating discussion.

Edited by: R. Volkamer

References

- Albarran, G. and Schuler, R.H.: Concerted effects in the reaction of OH radicals with aromatics: The cresols, *J. Phys. Chem. A*, 109, 9363–9370, 2005.
- Anastasi, C. and Smith, I. W. M.: Rate measurements of reactions of OH by resonance absorption. Part 6. – Rate constants for OH + NO(+M) → HNO₂(+M) over a wide range of temperature and pressure, *J. Chem. Soc. Faraday Trans. II*, 74, 1056–1064, 1978.
- Atkinson, R.: Kinetics and mechanisms of the gas-phase reactions of the hydroxyl radical with organic compounds, *J. Phys. Chem. Ref. Data*, Monograph No. 1, 1989.
- Atkinson, R.: Gas-phase tropospheric chemistry of organic compounds. A review, *Atmos. Environ.*, 24A, 1–41, 1990.
- Atkinson, R.: Gas-phase tropospheric chemistry of organic compounds, *J. Phys. Chem. Ref. Data*, Monograph No. 2, 1994.
- Atkinson, R.: Kinetics of the gas-phase reactions of OH radicals with alkanes and cycloalkanes. *Atmos. Chem. Phys.*, 3, 2233–2307, 2003, <http://www.atmos-chem-phys.net/3/2233/2003/>.
- Atkinson, R. and Aschmann, S. M.: Products of the gas-phase reactions of aromatic hydrocarbons: Effect of NO₂ concentration, *Int. J. Chem. Kinet.*, 26, 929–944, 1994.
- Atkinson, R. and Arey, J.: Atmospheric degradation of volatile organic compounds, *Chem. Rev.*, 103, 4605–4638, 2003.
- Atkinson, R., Aschmann, S. M., Arey, J., and Carter, W. P. L.: Formation of ring-retaining products from the OH radical-initiated reactions of benzene and toluene, *Int. J. Chem. Kinet.*, 21, 801–827, 1989.
- Atkinson, R., Aschmann, S.M., and Arey, J.: Formation of ring-retaining products from the OH-radical-initiated reactions of o-, m-, and p-xylene, *Int. J. Chem. Kinet.*, 23, 77–97, 1991.
- Behnke, W., Holländer, W., Koch, W., Nolting, F., and Zetzsch, C.: A smog chamber for studies of the photochemical degradation of chemicals in the presence of aerosols, *Atmos. Environ.*, 22, 1113–1120, 1988.
- Berho, F. and Lesclaux, R.: Gas-phase reactivity of the cyclohexadienyl radical *Phys. Chem. Chem. Phys.*, 3, 970–979, 2001.
- Berndt, T. and Böge, O.: Rate constants for the gas-phase reaction of hexamethylbenzene with OH radicals and H atoms and of 1,3,5-trimethylbenzene with H atoms, *Int. J. Chem. Kinet.*, 33, 124–129, 2001a.
- Berndt, T. and Böge, O.: Gas-phase reaction of OH radicals with benzene: products and mechanism, *Phys. Chem. Chem. Phys.*, 3, 4946–4956, 2001b.
- Berndt, T. and Böge, O.: Gas-phase reaction of OH radicals with phenol, *Phys. Chem. Chem. Phys.*, 5, 342–350, 2003.
- Berndt, T. and Böge, O.: Formation of phenol and carbonyls from the reaction of OH radicals with benzene, *Phys. Chem. Chem. Phys.*, 8, 1205–1214, 2006.
- Bethel, H., Atkinson, R., and Arey, J.: Products of the gas-phase reactions of OH radicals with p-xylene and 1,2,3- and 1,2,4-trimethylbenzene: Effect of NO₂ concentration, *J. Phys. Chem.*, A, 104, 8922–8929, 2000.
- Bjergbakke, E., Sillesen, A., and Pagsberg, P.: UV spectrum and kinetics of hydroxycyclohexadienyl radicals, *J. Phys. Chem.*, 100, 5729–5736, 1996, Comment by Koch, R., *J. Phys. Chem. B*, 101, 293, 1997.
- Bloss, C., Wagner, V., Bonzanini, A., Jenkin, M. E., Wirtz, K., Martin-Reviejo, M., and Pilling, M. J.: Evaluation of detailed aromatic mechanisms (MCMv3 and MCMv3.1) against environmental chamber data, *Atmos. Chem. Phys. Discuss.*, 4, 5683–5731, 2004, Interactive comment by Referee #2, *ibid.*, S2391–2395, 2004.
- Bohn, B.: Formation of peroxy radicals from OH–toluene adducts and O₂, *J. Phys. Chem. A*, 105, 6092–6101, 2001.
- Bohn, B. and Zetzsch, C.: Gas-phase reaction of the OH–benzene adduct with O₂: Reversibility and secondary formation of HO₂, *Phys. Chem. Chem. Phys.*, 1, 5097–5107, 1999.
- Bohn, B., Elend, M., and Zetzsch, C.: Abbaumechanismen von Aromaten nach Anlagerung von OH und ihr Einfluss auf die Kreisläufe von HO_x unter Bildung von Photooxidantien. LT3/TFS Jahresbericht, BMBF-Verbundvorhaben: Troposphärenforschungsschwerpunkt, Zwischenbericht 1999/Endbericht, Band 1: Prozessstudien, 217–227, 2000.
- Calvert, J. G., Atkinson, R., Becker, K. H., Kamens, R. M., Seinfeld, J. H., Wallington, T. H., and Yarwood, G.: The mechanisms of atmospheric oxidation of aromatic hydrocarbons, Oxford Univ. Press, 2002.

- Coeur-Tourneur, C., Henry, F., Janquin, M.-A., and Brutier, L.: Gas-phase reaction of hydroxyl radicals with m-, o- and p-cresol, *Int. J. Chem. Kinet.*, **38**, 553–562 (2006).
- Elend, M. and Zetzsch, C.: The influence of oxygen on the apparent rate constant for the reaction of OH with aromatics in smog chamber experiments in nitrogen at one atmosphere, in: Laboratory studies on atmospheric chemistry, air pollution research report 42 (Proc. CEC/EUROTRAC workshop, York 1991), CEC, Brussels, 123–126, 1992.
- Estupinan, E., Villenave, E., Raoult, S., Rayez, J. C., Rayez, M. T., and Lesclaux, R.: Kinetics and mechanism of the gas-phase reaction of the cyclohexadienyl radical c-C₆H₇ with O₂, *Phys. Chem. Chem. Phys.*, **5**, 4840–4845, 2003.
- Fang, X., Pan, X., Rahmann, A., Schuchmann, H.-P., and von Sonntag, C.: Reversibility in the reaction of cyclohexadienyl radicals with oxygen in aqueous solution, *Chem. Eur. J.*, **7**, 423–429, 1995.
- Ghigo, G. and Tonachini, G.: Benzene oxidation in the troposphere: theoretical investigation of the possible competition of three postulated reaction channels, *J. Amer. Chem. Soc.* **120**, 6753–6757, 1998.
- Goumri, A., Sawerysyn, J.-P., Pauwels, J.-F., and Devolder P.: Tropospheric oxidation of toluene: Reactions of some intermediate radicals, in: Physico-chemical behaviour of atmospheric pollutants, edited by: Restelli, G. and Angeletti, G., Kluwer Acad. Publ., Dordrecht, 315–319, 1990.
- Grebenkin, S. Y. and Krasnoperov, L. N.: Kinetics and thermochemistry of the hydroxycyclohexadienyl radical reaction with O₂: C₆H₆OH + O₂ → C₆H₆(OH)OO, *J. Phys. Chem. A*, **108**, 1953–1963, 2004.
- Hübner, G., and Roduner, E.: EPR investigation of HO· radical initiated degradation reactions of sulfonated aromatics as model compounds for fuel cell proton conducting membranes, *J. Mater. Chem.*, **9**, 409–418, 1999.
- Jenkin, M. E., Saunders, S. M., Wagner, V., and Pilling, M. J.: Protocol for the development of the Master Chemical Mechanism, MCM v3 (Part B): Tropospheric degradation of aromatic volatile organic compounds, *Atmos. Chem. Phys.*, **3**, 181–193, 2003, <http://www.atmos-chem-phys.net/3/181/2003/>.
- Johnson, D., Raoult, S., Rayez, M.-T., Rayez, J.-C., and Lesclaux, R.: An experimental and theoretical investigation of the gas-phase benzene–OH radical adduct + O₂ reaction, *Phys. Chem. Chem. Phys.*, **4**, 4678–4686, 2002.
- Johnson, D., Raoult, S., Lesclaux, R., and Krasnoperov, L.N.: UV absorption spectra of methyl-substituted hydroxycyclohexadienyl radicals in the gas phase, *J. Photochem. Photobiol. A*, **176**, 98–106, 2005.
- Klotz, B., Sörensen, S., Barnes, I., Becker, K.H., Etkorn, T., Volkamer, R., Platt, U., Wirtz, K., and Martin-Reviejo, M.: Atmospheric oxidation of toluene in a large-volume outdoor photoreactor: In situ determination of ring-retaining product yields, *J. Phys. Chem. A*, **110**, 10289–10299 (1998).
- Klotz, B., Volkamer, R., Hurley, M. D., Sulbaeck Andersen, M. P., Nielsen, O.J., Barnes, I., Imamura, T., Wirtz, K., Becker, K. H., Platt, U., Wallington, T. J., and Washida, N.: OH-initiated oxidation of benzene, Part II. Influence of elevated NO_x concentrations, *Phys. Chem. Chem. Phys.*, **4**, 4399–4411, 2002.
- Knispel, R., Koch, R., Siese, M., and Zetzsch, C.: Adduct formation of OH radicals with benzene, toluene, and phenol and consecutive reactions of the adducts with NO_x and O₂, *Ber. Bunsenges. Phys. Chem.*, **94**, 1375–1379, 1990.
- Koch, R.: Kinetische Untersuchung der Folgereaktionen der OH-Addukte mit NO, NO₂ und O₂ mit simultaner Auswertung von Kurvenscharen, PhD thesis, Univ. of Hannover, 1992.
- Koch, R. and Zetzsch, C.: Cycling of OH radicals in the system naphthalene/O₂/NO studied by FP/RF and LP/RF, presented at the 13th Int. Sympos. on Gas Kinetics, Dublin, 1994.
- Koch, R. and Zetzsch, C.: First experimental evidence of ipso addition of OH to methyl-substituted aromatics and O₂ reactivity of hexamethylbenzene–OH, poster contribution to the Bunsen Conference, Erlangen, Germany, 2006, available at www.bayceer.uni-bayreuth.de/atchem/data/aro_ref/bunsen_poster06.ppt.
- Koch, R., Knispel, R., Siese, M., and Zetzsch, C.: Absolute rate constants and products of secondary steps in the atmospheric degradation of aromatics, in: Physico-chemical behaviour of atmospheric pollutants, edited by: Angeletti, G. and Restelli, G., European Commission, Brussels/Luxemburg, 143–149, 1994.
- Koch, R., Bohn, B., and Zetzsch, C.: Cycles of HO_x as a tool to investigate the tropospheric chemistry of aromatics in kinetic experiments, in: The oxidizing capacity of the troposphere, physico-chemical behaviour of atmospheric pollutants, edited by: Larsen, B., Versino, B., and Angeletti, G., European Commission, Brussels, 217–221, 1997.
- Lay, T. H., Bozzelli, J. W., and Seinfeld, J. H.: Atmospheric photochemical oxidation of benzene: Benzene + OH and the benzene–OH adduct (hydroxyl-2,4-cyclohexadienyl) + O₂, *J. Phys. Chem.*, **100**, 6543–6554, 1996.
- Michael, J. V., Nava, D. F., Payne, W. A., Lee, J. H., and Stief, L. J.: Rate constant for the reaction atomic hydrogen + nitrogen dioxide from 195 to 400 K with FP-RF and DF-RF techniques, *J. Phys. Chem.*, **83**, 2818–2823, 1979.
- Monks, P. S., Carpenter, L. J., Penkett, S. A., Ayers, G. P., Gillett, R. W., Galbally, I. E., and Meyer, C. P. (Mick): Fundamental ozone photochemistry in the remote marine boundary layer: The SOAPEX experiment, measurement and theory, *Atmos. Environ.*, **32**, 3647–3664, 1998.
- Mvula, E., Schuchmann, M.N., von Sonntag, C.: Reactions of phenol-OH-adduct radicals. Phenoxy radical formation by water elimination vs. oxidation by dioxygen. *J. Chem. Soc., Perkin Trans.*, **2**, 264–268, 2001.
- Nolting, F., Behnke, W., and Zetzsch, C.: A smog chamber for studies of the reactions of terpenes and alkanes with ozone and OH, *J. Atmos. Chem.*, **6**, 47–59, 1988.
- Olariu, R.I., Klotz, B., Barnes, I., Becker, K.H., and Mocanu, R.: FT-IR study of the ring-retaining products from the reaction of OH radicals with phenol, o-, m-, and p-cresol, *Atmos. Environ.*, **36**, 3685–3697, 2002.
- Pan, X.-M. and von Sonntag, C.: Hydroxyl-radical-induced oxidation of benzene in the presence of oxygen: R· + O₂ ↔ RO₂· equilibria in aqueous solution. A pulse radiolysis study, *Zeitschrift für Naturforschung, B: Chemical Sciences*, **45**, 1337–1340, 1990.
- Pan, X.-M., Schuchmann, M.N., and von Sonntag, C.: Oxidation of benzene by the OH radical. A product and pulse radiolysis study, *J. Chem. Soc., Perkin Trans 2*, 289–297, 1993.
- Paraskevopoulos, G. and Singleton, D. L.: Reactions of OH radicals with inorganic compounds in the gas phase, *Rev. Chem.*

- Intermed., 10, 139–218, 1988.
- Peller, J., Wiest, O., and Kamat, P. V.: Mechanism of hydroxyl radical-induced breakdown of the herbicide 2,4-dichlorophenoxyacetic acid (2,4-D), *Chem. Eur. J.*, 9, 5379–5387, 2003.
- Perry, R. A., Atkinson, R., and Pitts, Jr. J. N.: Kinetics and mechanism of the gas phase reaction of OH radicals with aromatic hydrocarbons over the temperature range 296–473 K, *J. Phys. Chem.*, 81, 296–304, 1977.
- Press, W. H., Teukolsky, S. A., Vetterling, W. T., and Flannery, B. P.: Numerical recipes in FORTRAN: The Art of Scientific Computing, Cambridge Univ. Press, 1992.
- Raff, J. D. and Hites, R. A.: Gas-Phase Reaction of Brominated Diphenylethers with OH Radicals, *J. Phys. Chem. A*, 110, 10783–10792, 2006.
- Raoult, S., Rayez, M.-T., Rayez, J.-C., and Lesclaux, R.: Gas-phase oxidation of benzene: Kinetics, thermochemistry and mechanism of initial steps, *Phys. Chem. Chem. Phys.*, 6, 2245–2253, 2004.
- Richter, H. W. and Waddell, W. H.: Mechanism of the oxidation of dopamine by the hydroxyl radical in aqueous solution, *J. Am. Chem. Soc.*, 105, 5434–5440, 1983.
- Rinke, M. and Zetzsch, C.: Rate constants for the reactions of OH-radicals with aromatics: benzene, phenol, aniline and 1,2,4-trichlorobenzene, *Ber. Bunsenges. Phys. Chem.*, 88, 55–62, 1984.
- Schuler, R. H., Albarran, G., Zajicek, J., George, M. V., Fessenden, R. W., and Carmichael, I.: On the addition of ·OH radicals to the ipso positions of alkyl-substituted aromatics: Production of 4-hydroxy-4-methyl-2,5-cyclohexadien-1-one in the radiolytic oxidation of p-cresol, *J. Phys. Chem. A*, 106, 12178–12183, 2002.
- Smith, D.F., McIver, C.D., and Kleindienst, T.: Primary product distribution from the reaction of hydroxyl radicals with toluene at ppb NO_x mixing ratios, *J. Atmos. Chem.*, 30, 209–228, 1998.
- Smith, D.F., Kleindienst, T., and McIver, C.: Primary product distribution from the reaction of OH with m-, p-xylene, 1,2,4- and 1,3,5-trimethylbenzene, *J. Atm. Chem.*, 34, 339–364, 1999.
- Solar, S., Solar, W., and Getoff, N.: Resolved multisite OH-attack on aqueous aniline studied by pulse radiolysis, *Radiat. Phys. Chem.* 2, 229–234, 1986.
- Stephenson, R.M. and Malanowski, S.: Handbook of the thermodynamics of organic compounds. Elsevier, New York 1987.
- Stuhl, F. and Niki, H.: Flash photochemical study of the reaction OH+NO+M using resonance fluorescent detection of OH, *J. Chem. Phys.*, 57, 3677–3679, 1972.
- Suh, I., Zhang, D., Zhang, R., Molina, L. T., and Molina, M. J.: Theoretical study of OH addition reaction to toluene, *Chem. Phys. Lett.*, 364, 454–462, 2002.
- Volkamer, R., Klotz, B., Barnes, I., Imamura, T., Wirtz, K., Washida, H., Becker, K.H., Platt, U.: OH-initiated oxidation of benzene Part I. Phenol formation under atmospheric conditions. *Phys. Chem. Chem. Phys.*, 4, 1598–1610, 2002a.
- Volkamer, R., Uecker, J., Wirtz, K., and Platt, U.: OH-radical initiated oxidation of BTXM: Fate of phenol-type compounds in the presence of NO_x, Proceedings from the EUROTRAC-2 Symposium 2002, edited by: Midgley, P.M. and Reuther, M., Margraf Verlag, Weikersheim, 2002b.
- Wagner, H. G., Welzbacher, U., and Zellner, R.: Rate measurements for the reactions H + NO₂ → OH + NO and H + NOCl → HCl + NO by Lyman-alpha fluorescence, *Ber. Bunsenges. Phys. Chem.*, 80, 1023–1027, 1976.
- Wahner, A. and Zetzsch, C.: Rate constants for the addition of OH to aromatics (benzene, p-chloroaniline and o-, m- and p-dichlorobenzene) and the unimolecular decay of the adduct. Kinetics into a quasi-equilibrium, *J. Phys. Chem.*, 87, 4945–4951, 1983.
- Wallington, T. J., Neuman, D. M., and Kurylo, M. J.: Kinetics of the gas phase reaction of hydroxyl radicals with ethane, benzene and a series of halogenated benzenes over the temperature range 234–438 K, *Int. J. Chem. Kinet.*, 19, 725–739, 1987.
- Witte, F., Urbanik, E., and Zetzsch, C.: Temperature dependence of the rate constants for the addition of OH to benzene and to some monosubstituted aromatics (aniline, bromobenzene and nitrobenzene) and the unimolecular decay of the adducts. Kinetics into a quasi-equilibrium 2, *J. Phys. Chem.*, 90, 3251–3259, 1986.
- Witte, F. and Zetzsch, C.: Annual report of the steering committee of LACTOZ, a joint EUROTRAC/COST 611 project, EU-REKA/CEC, Brussels, 62–66, 1988.
- Zellner, R., Fritz, B., and Preidel, M.: A cw UV laser absorption study of the reactions of the hydroxy-cyclohexadienyl radical with NO₂ and NO, *Chem. Phys. Lett.*, 121, 412–416, 1985.
- Zetzsch, C., Koch, R., Siese, M., Witte, F., and Devolder, P.: Adduct formation of OH with benzene and toluene and reaction of the adducts with NO and NO₂, in: Physico-Chemical Behaviour of Atmospheric Pollutants, edited by: Restelli, G. and Angeletti, G., Kluwer Acad. Publ., Dordrecht, 320–327, 1990.
- Zetzsch, C., Koch, R., Bohn, B., Knispel, R., Siese, M., and Witte, F.: Adduct formation of OH with aromatics and unsaturated hydrocarbons and consecutive reactions with O₂ and NO_x to regenerate OH, in: Chemical Processes in Atmospheric Oxidation, edited by: Le Bras, G., Springer, Berlin, 1997, 247–256.
- Zhao, J., Zhang, R., Misawa, K., and Shibuya, K.: Experimental product study of the OH-initiated oxidation of m-xylene, *J. Photochem. Photobiol. A: Chemistry*, 176, 199–207, 2005.